

Crossover from first- to second-order transition in frustrated Ising antiferromagnetic films

X. T. Pham Phu,¹ V. Thanh Ngo,² and H. T. Diep^{1,*}

¹*Laboratoire de Physique Théorique et Modélisation, Université de Cergy-Pontoise, CNRS, UMR 8089 2, Avenue Adolphe Chauvin, 95302 Cergy-Pontoise, France*

²*Institute of Physics, VAST, P.O. Box 429, Bo Ho, Hanoi 10000, Vietnam*
(Received 24 February 2009; published 9 June 2009)

In the bulk state, the Ising face-centered-cubic (fcc) antiferromagnet is fully frustrated and is known to have a very strong first-order transition. In this paper, we study the nature of this phase transition in the case of a thin film as a function of the film thickness. Using Monte Carlo simulations, we show that the transition remains first order down to a thickness of four fcc cells (eight atomic layers). It becomes clearly second order at a thickness of two fcc cells, i.e., four atomic layers. It is also interesting to note that the presence of the surface reduces the ground-state degeneracy found in the bulk. For the two-cell thickness, the surface magnetization is larger than the interior one. It undergoes a second-order phase transition at a temperature T_C while interior spins become disordered at a lower temperature T_D . This loss of order is characterized by a peak of the interior spins susceptibility and a peak of the specific heat which do not depend on the lattice size suggesting that either it is not a real transition or it is a Kosterlitz-Thouless nature. The surface transition, on the other hand, is shown to be of second order with critical exponents deviated from those of pure two-dimensional Ising universality class. We also show results obtained from the Green's function method. A discussion is given.

DOI: [10.1103/PhysRevE.79.061106](https://doi.org/10.1103/PhysRevE.79.061106)

PACS number(s): 75.10.-b, 75.40.Mg, 75.70.Rf

I. INTRODUCTION

This paper deals with the question whether or not the phase transition known in the bulk state changes its nature when the system is made as a thin film. In a recent work, we have considered the case of a bulk second-order transition. We have shown that under a thin-film shape, i.e., with a finite thickness, the transition shows effective critical exponents whose values are between two-dimensional (2D) and three-dimensional (3D) universality classes [1]. If we scale these values with a function of thickness as suggested by Fisher [2] we should find, as long as the thickness is finite, the 2D universality class.

In this paper, we study the effect of the film thickness in the case of a bulk first-order transition. The question to which we would like to answer is whether or not the first order becomes a second order when reducing the thickness. For that purpose we consider the face-centered-cubic (fcc) Ising antiferromagnet. This system is fully frustrated with a very strong first-order transition.

On the one hand, effects of the frustration in spin systems have been extensively investigated during the last 30 years. In particular, by exact solutions, we have shown that frustrated spin systems have rich and interesting properties such as successive phase transitions with complicated nature, partial disorder, reentrance, and disorder lines [3,4]. Frustrated systems still challenge theoretical and experimental methods. For recent reviews, the reader is referred to Ref. [5].

On the other hand, physics of surfaces and objects of nanometric size have also attracted an immense interest. This is due to important applications in industry [6–8]. In this field, research results are often immediately used for industrial applications without waiting for a full theoretical under-

standing. An example is the so-called giant magnetoresistance used in data storage devices, magnetic sensors, etc. [9–12]. In parallel to these experimental developments, much theoretical effort has also been devoted to the search of physical mechanisms lying behind new properties found in nanometric objects such as ultrathin films, ultrafine particles, quantum dots, spintronic devices, etc. This effort aimed not only at providing explanations for experimental observations but also at predicting new effects for future experiments [13,14].

The above-mentioned aim of this paper is thus to investigate the combined effects of frustration and film thickness which are expected to be interesting because of the symmetry reduction. As said above, the bulk fcc Ising antiferromagnet is fully frustrated because it is composed of tetrahedra whose faces are equilateral triangles. The antiferromagnetic (AF) interaction on such triangles causes a full frustration [5]. The bulk properties of this material have been largely studied as we will show below. In this paper, we shall use the recent high precision technique called “Wang-Landau” flat histogram Monte Carlo (MC) simulations to identify the order of the transition. We also use the Green's function (GF) method for qualitative comparison.

The paper is organized as follows. Section II is devoted to the description of the model. We recall there properties of the 3D counterpart model in order to better appreciate properties of thin films obtained in this paper. In Sec. III, we show our results obtained by MC simulations on the order of the transition. A detailed discussion on the nature of the phase transition is given. In the regime of second-order transition, we show in this section the results on the critical exponents obtained by MC flat histogram technique. Section IV is devoted to a study of the quantum version of the same model by the use of the GF method. Concluding remarks are given in Sec. V.

*Corresponding author; diep@u-cergy.fr

II. MODEL AND GROUND-STATE ANALYSIS

It is known that the AF interaction between nearest-neighbor (NN) spins on the fcc lattice causes a very strong frustration. This is due to the fact that the fcc lattice is composed of tetrahedra each of which has four equilateral triangles. It is well known [5] that it is impossible to fully satisfy simultaneously the three AF bond interactions on each triangle. In the case of Ising model, the ground state (GS) is infinitely degenerate for an infinite system size: on each tetrahedron two spins are up and the other two are down. The fcc system is composed of edge-sharing tetrahedra. Therefore, there is an infinite number of ways to construct the infinite crystal. The minimum number of ways of such a construction is a stacking, in one direction, of uncorrelated AF planes. The minimum GS degeneracy of a L^3 fcc-cell system (L being the number of cells in each direction) is therefore equal to 3×2^{2L} where the factor 3 is the number of choices of the stacking direction, 2 the degeneracy of the AF spin configuration of each plane, and $2L$ the number of atomic planes in one direction of the fcc crystal (the total number of spins is $N=4L^3$). The GS degeneracy is therefore of the order of $2^{N^{1/3}}$. Note that at finite temperature, due to the so-called “order by disorder” [15,16], the spins will choose a long-range ordering. In the case of AF fcc Ising crystal, this ordering is an alternate stacking of up-spin planes and down-spin planes in one of the three directions. This has been observed also in the Heisenberg case [17] as well as in other frustrated systems [18].

The phase transition of the bulk frustrated fcc Ising antiferromagnet has been found to be of the first order [19–23]. Note that for the Heisenberg model, the transition is also found to be of the first order as in the Ising case [17,24]. Other similar frustrated antiferromagnets such as the hcp XY and Heisenberg antiferromagnets [25] and stacked triangular XY and Heisenberg antiferromagnets [26,27] show the same behavior.

Let us consider a film of fcc lattice structure with (001) surfaces. The Hamiltonian is given by

$$\mathcal{H} = - \sum_{\langle i,j \rangle} J_{i,j} \sigma_i \cdot \sigma_j, \quad (1)$$

where σ_i is the Ising spin at the lattice site i ; $\sum_{\langle i,j \rangle}$ indicates the sum over the NN spin pairs σ_i and σ_j .

In the following, the interaction between two NN on the surface is supposed to be AF and equal to J_s . All other interactions are equal to $J=-1$ for simplicity. Note that in a previous paper [28], we have studied the case of the Heisenberg model on the same fcc AF film as a function of J_s .

For Ising spins, the GS configuration can be determined in a simple way as follows: we calculate the energy of the surface spin in the two configurations shown in Fig. 1 where the film surface contains spins 1 and 2 while the beneath layer spins 3 and 4. In the ordering of type I [Fig. 1(a)], the spins on the surface (xy plane) are antiparallel and in the ordering of type II [Fig. 1(b)] they are parallel. Of course, apart from the overall inversion, for type I there is a degenerate configuration by exchanging the spins 3 and 4. To see which con-

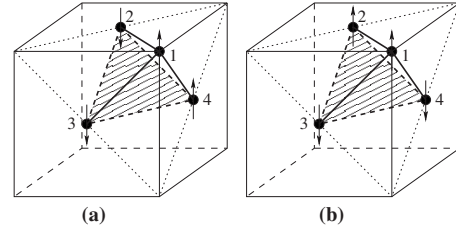


FIG. 1. The ground-state spin configuration of the fcc cell at the film surface: (a) ordering of type I for $J_s < -0.5|J|$; (b) ordering of type II for $J_s > -0.5|J|$.

figuration is stable, we write the energy of a surface spin for these two configurations,

$$E_I = -4|J_s|,$$

$$E_{II} = 4|J_s| - 4|J|. \quad (2)$$

One sees that $E_I \leq E_{II}$ when $J_s/J \geq 0.5$. In the following, we study the case $J_s = J = -1$ so that the GS configuration is of type I.

III. MONTE CARLO RESULTS

In this section, we show the results obtained by MC simulations with Hamiltonian (1) using the high-precision Wang-Landau flat histogram technique [29]. Wang and Landau recently proposed a MC algorithm for classical statistical models. The algorithm uses a random walk in energy space in order to obtain an accurate estimate for the density of states $\rho(E)$ which is defined as the number of spin configurations for any given E . This method is based on the fact that a flat energy histogram $H(E)$ is produced if the probability for the transition to a state of energy E is proportional to $\rho(E)^{-1}$. At the beginning of the simulation, the density of states (DOS) is set equal to 1 for all possible energies, $\rho(E)=1$. We begin a random walk in energy space (E) by choosing a site randomly and flipping its spin with a probability proportional to the inverse of the momentary density of states. In general, if E and E' are the energies before and after a spin is flipped, the transition probability from E to E' is

$$p(E \rightarrow E') = \min[\rho(E)/\rho(E'), 1]. \quad (3)$$

Each time an energy level E is visited, the DOS is modified by a modification factor $f > 0$ whether the spin flipped or not, i.e., $\rho(E) \rightarrow \rho(E)f$. At the beginning of the random walk, the modification factor f can be as large as $e^1 \approx 2.7182818$. A histogram $H(E)$ records how often a state of energy E is visited. Each time the energy histogram satisfies a certain “flatness” criterion, f is reduced according to $f \rightarrow \sqrt{f}$ and $H(E)$ is reset to zero for all energies. The reduction process of the modification factor f is repeated several times until a final value f_{final} which is close enough to 1. The histogram is considered as flat if

$$H(E) \geq x\% \cdot \langle H(E) \rangle \quad (4)$$

for all energies, where $x\%$ is chosen between 70% and 95% and $\langle H(E) \rangle$ is the average histogram.

The thermodynamic quantities [29,30] can be evaluated by

$$\langle E^n \rangle = \frac{1}{Z} \sum_E E^n \rho(E) \exp(-E/k_B T),$$

$$C_v = \frac{\langle E^2 \rangle - \langle E \rangle^2}{k_B T^2},$$

$$\langle M^n \rangle = \frac{1}{Z} \sum_E M^n \rho(E) \exp(-E/k_B T),$$

$$\chi = \frac{\langle M^2 \rangle - \langle M \rangle^2}{k_B T},$$

where Z is the partition function defined by

$$Z = \sum_E \rho(E) \exp(-E/k_B T). \quad (5)$$

The canonical distribution at any temperature can be calculated simply by

$$P(E, T) = \frac{1}{Z} \rho(E) \exp(-E/k_B T). \quad (6)$$

In this work, we consider a energy range of interest [31,32] (E_{\min}, E_{\max}). We divide this energy range to R subintervals, the minimum energy of each subinterval is E_{\min}^i for $i=1, 2, \dots, R$, and maximum of the subinterval i is $E_{\max}^i = E_{\min}^{i+1} + 2\Delta E$, where ΔE can be chosen large enough for a smooth boundary between two subintervals. The Wang-Landau algorithm is used to calculate the relative DOS of each subinterval (E_{\min}^i, E_{\max}^i) with the modification factor $f_{\text{final}} = \exp(10^{-9})$ and flatness criterion $x\% = 95\%$. We reject the suggested spin flip and do not update $\rho(E)$ and the energy histogram $H(E)$ of the current energy level E if the spin-flip trial would result in an energy outside the energy segment. The DOS of the whole range is obtained by joining the DOS of each subinterval ($E_{\min}^i + \Delta E, E_{\max}^i - \Delta E$).

The film size used in our present work is $L \times L \times N_z$, where L is the number of cells in x and y directions, while N_z is that along the z direction (film thickness). We use here $L = 30, 40, \dots, 150$ and $N_z = 2, 4, 8, 12$. Periodic boundary conditions are used in the xy planes. Our computer program was parallelized and run on a rack of several dozens of 64-bit CPU. $|J| = 1$ is taken as unit of energy in the following.

Before showing the results let us adopt the following notations. Sublattices 1 and 2 of the first fcc cell belong to the surface layer, while sublattices 3 and 4 of the first cell belong to the second layer [see Fig. 1(a)]. In our simulations, we used N_z fcc cells, i.e., $2N_z$ atomic layers. We used the symmetry of the two film surfaces.

A. Crossover of the phase transition

As said earlier, the bulk fcc antiferromagnet with Ising spins shows a very strong first-order transition. This is seen in MC simulation: Fig. 2 shows the energy per spin E versus

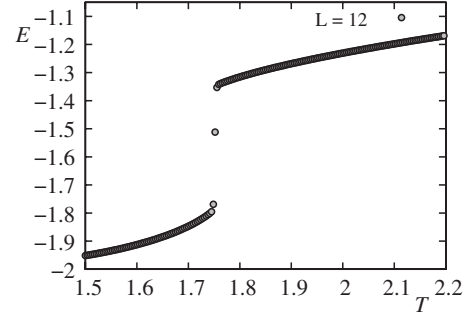


FIG. 2. Bulk energy vs T for $L=N_z=12$.

T for $L=N_z=12$. One observes here a very large latent heat indicating a strong first-order character even with a small lattice size. Using the density of states $\rho(E)$ obtained by the WL technique described above, we calculate the energy distribution with Eq. (6) for two cases: with and without periodic boundary conditions (PBC) in the z direction, at their respective transition temperatures $T_c = 1.75113$ and $T_c = 1.76849$ for the simulated size $L=N_z=12$ (Fig. 3). We observe here a double-peak structure confirming the first-order transition.

Our purpose here is to see whether the transition becomes second order when we decrease the film thickness. As it turns out, the transition remains of first order down to $N_z=4$ as seen by the double-peak energy distribution displayed in Fig. 4. Note that we do not need to go to larger L , since the transition is clearly of first order already at $L=40$. We can extrapolate these results to get the latent heat at the thermodynamic limit.

In Fig. 5 we plot the latent heat ΔE at $L \rightarrow \infty$ as a function of thickness N_z . Data points are well fitted with the following formula:

$$\Delta E = A - \frac{B}{N_z^{d-1}} \left[1 + \frac{C}{N_z} \right], \quad (7)$$

where $d=3$ is the dimension, $A=0.3370$, $B=3.7068$, $C=-0.8817$. Note that the term N_z^{d-1} corresponds to the surface separating two domains of ordered and disordered phases at the transition. The second term in the brackets corresponds to

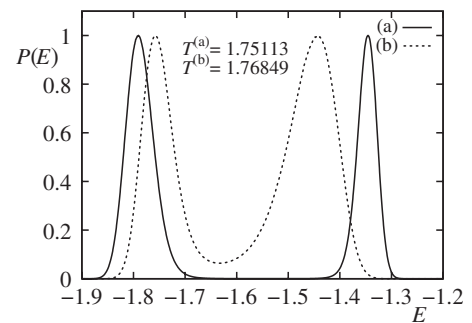


FIG. 3. Bulk energy distribution with periodic boundary conditions in all three directions (a) and without PBC in z direction. (b) The energy distribution was calculated using Eq. (6) for $L=N_z=12$ in the cases (a) and (b) at their respective transition temperatures $T_c = 1.75113$ and $T_c = 1.76849$.

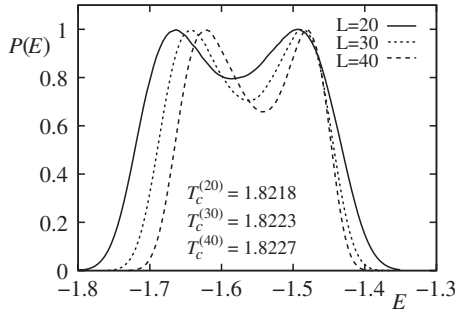


FIG. 4. Energy distribution for $L=20, 30, 40$ with film thickness $N_z=4$ (eight atomic layers) calculated using Eq. (6) at the transition temperatures $T=1.8218, 1.8223, 1.8227$, for these sizes, respectively.

a size correction. As seen in Fig. 5, the latent heat vanishes at a thickness between 2 and 3. This is verified by our simulations for $N_z=2$. For $N_z=2$ we find a transition with all second-order features: no discontinuity in energy (no double-peak structure) even when we go up to $L=150$.

Before showing in the following the results of $N_z=2$, let us discuss on the crossover. In the case of a film with finite thickness studied here, it appears that the first-order character is lost for very small N_z . A possible cause for the loss of the first-order transition is from the role of the correlation in the film. If a transition is of first order in 3D, i.e., the correlation length is finite at the transition temperature, then in thin films the thickness effect may be important: if the thickness is larger than the correlation length at the transition, then the first-order transition should remain. On the other hand, if the thickness is smaller than that correlation length, the spins then feel an “infinite” correlation length across the film thickness resulting in a second-order transition.

B. Film with four atomic layers ($N_z=2$)

Let us show in Figs. 6 and 7 the energy and the magnetizations of sublattices 1 and 3 of the first two cells with $L=120$ and $N_z=2$. It is interesting to note that the surface layer has larger magnetization than that of the second layer. This is not the case for nonfrustrated films where the surface magnetization is always smaller than the interior ones because of the effects of low-lying energy surface-localized magnon modes [33,34]. One explanation can be advanced: due to the

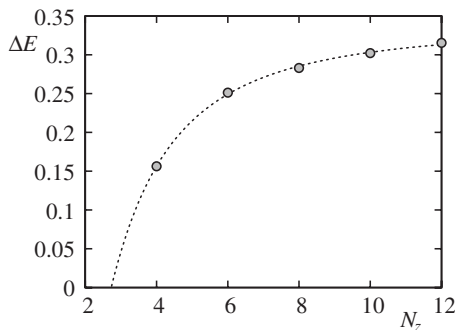


FIG. 5. The latent heat ΔE extrapolated at $L \rightarrow \infty$ as a function of thickness N_z .

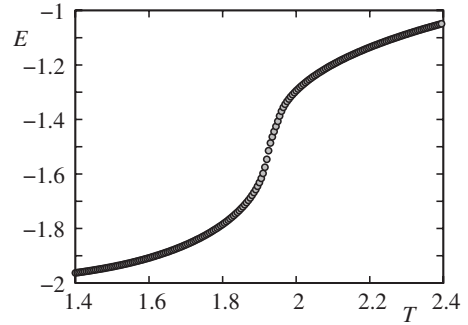


FIG. 6. Energy versus temperature T for $L=120$ with film thickness $N_z=2$.

lack of neighbors surface spins are less frustrated than the interior spins. As a consequence, the surface spins maintain their ordering up to a higher temperature.

Let us discuss finite-size effects in the transitions observed in Figs. 8 and 9. This is an important question because it is known that some apparent transitions are artifacts of small system sizes. To confirm further the observed transitions, we have made a study of finite-size effects on the layer susceptibilities by using the Wang-Landau technique described above [29].

We observe that there are two peaks in the specific heat: the first peak at $T_1 \approx 1.927$, corresponding to the vanishing of the sublattice magnetization 3, does not depend on the lattice size while the second peak at $T_2 \approx 1.959$, corresponding to the vanishing of the sublattice magnetization 1, does depend on L . Both energy distributions calculated at these temperatures and the nearby ones show a Gaussian form indicating a non-first-order transition (see Fig. 10).

The fact that the peak at T_1 does not depend on L suggests two scenarios: (i) the peak does not correspond to a real transition, since there exist systems where C_v shows a peak but we know that there is no transition just as in the case of one-dimensional Ising chain; (ii) the peak corresponds to a Kosterlitz-Thouless transition. To confirm this we need to check carefully several points such as the behavior of the correlation length, etc. This is a formidable task which is not the scope of this work.

Whatever the scenario for the origin of the peak at T_1 , we know that the interior layers are disordered between T_1 and T_2 , while the two surface layers are still ordered. Thus, the

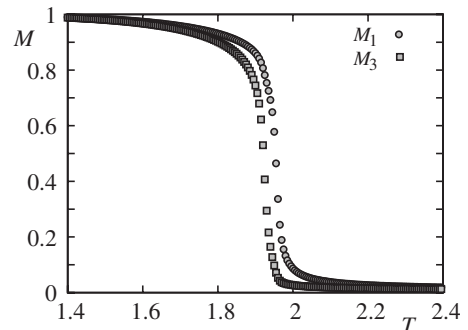


FIG. 7. Sublattice magnetization for $L=120$ with film thickness $N_z=2$.

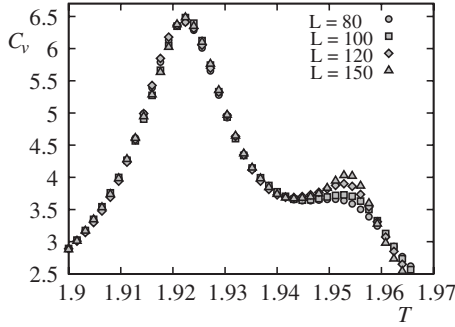


FIG. 8. Specific heats are shown for various sizes L as a function of temperature.

transition of the surface layers occurs while the disordered interior spins act on them as dynamical random fields. Unlike the true 2D random-field Ising model, which does not allow a transition at finite temperature [35], the random fields acting on the surface layer are correlated. This explains why one has a finite- T transition here. Note that this situation is known in some exactly solved models where partial disorder coexists with order at finite T [3,4,36]. However, it is not obvious to foresee what is the universality class of the transition at T_2 . The theoretical argument of Capelhart and Fisher [2] does not apply in the present situation because one does not have a single transition here, unlike the case of simple cubic ferromagnetic films studied before [1]. So, we wish to calculate the critical exponents associated with the transition at T_2 .

The exponent ν can be obtained as follows. We calculate as a function of T the magnetization derivative with respect to $\beta=(k_B T)^{-1}$: $V_1 = \langle (\ln M)' \rangle = \langle E \rangle - \langle ME \rangle / \langle M \rangle$, where E is the system energy and M is the sublattice order parameter. We identify the maximum of V_1 for each size L . From the finite-size scaling we know that V_1^{\max} is proportional to $L^{1/\nu}$

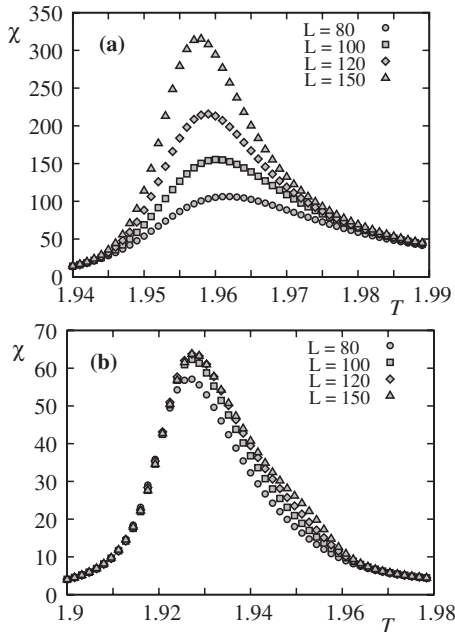


FIG. 9. Susceptibilities of sublattices (a) 1 and (b) 3 are shown for various sizes L as a function of temperature.

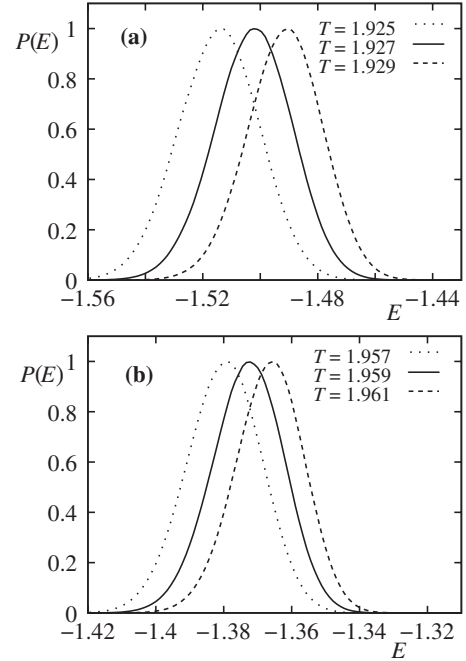


FIG. 10. Energy distributions for $L=120$ with film thickness $N_z=2$ at the two temperatures (solid lines) corresponding to the peaks observed in the specific heat. Other curves are those at nearby temperatures. See text for comment.

[37]. We show in Fig. 11 the maximum of V_1 versus $\ln L$ for the first layer. We find $\nu=0.887 \pm 0.009$. Now, using the scaling law $\chi^{\max} \propto L^{\gamma/\nu}$, we plot $\ln \chi^{\max}$ versus $\ln L$ in Fig. 12. The ratio of the critical exponents γ/ν is obtained by the slope of the straight line connecting the data points of each layer. From the value of ν we obtain $\gamma=1.542 \pm 0.005$. These values do not correspond neither to 2D nor 3D Ising models ($\gamma_{2D}=1.75$, $\nu_{2D}=1$, $\gamma_{3D}=1.241$, $\nu_{3D}=0.63$). We note however that if we think of the weak universality where only ratios of critical exponents are concerned [38], then the ratios of these exponents $1/\nu=1.128$ and $\gamma/\nu=1.739$ are not far from the 2D ones which are 1 and 1.75, respectively.

IV. GREEN'S FUNCTION METHOD

We consider here the same fcc system but with quantum Heisenberg spins. To compare the results with the Ising case, we add in the Hamiltonian an Ising-type anisotropy interac-

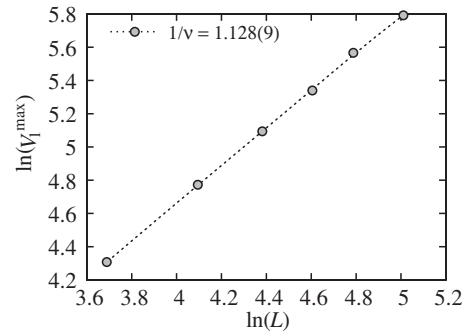


FIG. 11. The maximum value of $V_1 = \langle E \rangle - \langle ME \rangle / \langle M \rangle$ versus L in the \ln - \ln scale. The slope of this straight line gives $1/\nu$. Error bars are smaller than the size of the data points.

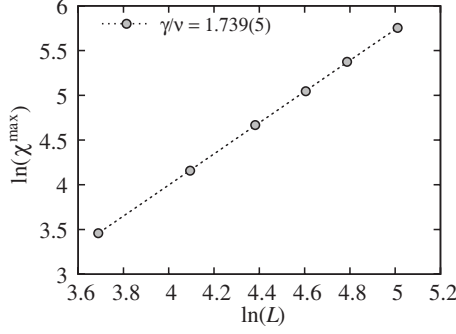


FIG. 12. Maximum sublattice susceptibility χ^{\max} versus L in the ln-ln scale. The slope of this straight line gives γ/v . Error bars are smaller than the size of the data points.

tion term. In addition, this term avoids the absence of long-range order of isotropic non-Ising spin model at finite temperature (T) when the film thickness is very small, i.e., quasi-two-dimensional system [39]. The Hamiltonian is given by

$$\mathcal{H} = - \sum_{\langle i,j \rangle} J_{i,j} \mathbf{S}_i \cdot \mathbf{S}_j - \sum_{\langle i,j \rangle} I_{i,j} S_i^z S_j^z, \quad (8)$$

where \mathbf{S}_i is the Heisenberg spin at the lattice site i ; $\sum_{\langle i,j \rangle}$ indicates the sum over the NN spin pairs \mathbf{S}_i and \mathbf{S}_j . $J_{i,j}$ and $I_{i,j}$ are antiferromagnetic (negative). Note that in the laboratory coordinates, the up spins have $S^z \geq 0$ while the down spins have $S^z \leq 0$.

We can rewrite Hamiltonian (8) in the relative local spin coordinates as

$$\begin{aligned} \mathcal{H} = & - \sum_{\langle i,j \rangle} J_{i,j} \left\{ \frac{1}{4} (\cos \theta_{ij} - 1) (S_i^+ S_j^+ + S_i^- S_j^-) + \frac{1}{4} (\cos \theta_{ij} + 1) \right. \\ & \times (S_i^+ S_j^- + S_i^- S_j^+) + \frac{1}{2} \sin \theta_{ij} (S_i^+ + S_i^-) S_j^z \\ & \left. - \frac{1}{2} \sin \theta_{ij} S_i^z (S_j^+ + S_j^-) + \cos \theta_{ij} S_i^z S_j^z \right\} - \sum_{\langle i,j \rangle} I_{i,j} \cos \theta_{ij} S_i^z S_j^z, \end{aligned} \quad (9)$$

where θ_{ij} is the angle between two NN spins. Note that in the above expression, we have transformed all $S^z \geq 0$; the relative spin orientation of each spin pair is now expressed by θ_{ij} . In a collinear spin configuration such as those shown in Fig. 1, $\cos \theta_{ij} = -1$ and 1 for antiparallel and parallel pairs, respectively, while $\sin \theta_{ij} = 0$. In noncollinear structures, the calculation is more complicated. The general GF method for noncollinear spin configuration has been proposed elsewhere [40,41]. In the present study, one has a collinear spin configuration shown in Fig. 1 because of the Ising-type anisotropy. We define two double-time GF by

$$G_{ij}(t, t') = \langle \langle S_i^+(t); S_j^-(t') \rangle \rangle, \quad (10)$$

$$F_{mj}(t, t') = \langle \langle S_m^-(t); S_j^-(t') \rangle \rangle. \quad (11)$$

where i and j belong to the up-spin sublattice, and m to the down-spin one. In the case of thin films, the reader is referred to Refs. [28,33,34] for a general formulation. We de-

scribe here only the main steps: we first write the equations of motion for $G_{ij}(t, t')$ and $F_{mj}(t, t')$ and we next neglect higher-order correlations by using the Tyablikov decoupling scheme [42] which is known to be valid for exchange terms [43], and then we introduce the following Fourier transforms in the xy plane:

$$G_{i,j}(t, t') = \frac{1}{\Delta} \int \int d\mathbf{k}_{xy} \frac{1}{2\pi} \int_{-\infty}^{+\infty} d\omega e^{-i\omega(t-t')} \times g_{n,n'}(\omega, \mathbf{k}_{xy}) e^{i\mathbf{k}_{xy} \cdot (\mathbf{R}_i - \mathbf{R}_j)}, \quad (12)$$

$$F_{m,j}(t, t') = \frac{1}{\Delta} \int \int d\mathbf{k}_{xy} \frac{1}{2\pi} \int_{-\infty}^{+\infty} d\omega e^{-i\omega(t-t')} \times f_{n,n'}(\omega, \mathbf{k}_{xy}) e^{i\mathbf{k}_{xy} \cdot (\mathbf{R}_m - \mathbf{R}_j)}, \quad (13)$$

where ω is the spin-wave frequency, \mathbf{k}_{xy} denotes the wave vector parallel to xy planes, \mathbf{R}_i is the position of the spin at the site i , n and n' are, respectively, the indices of the layers where the sites i (or m) and j belong to. One has $n, n' = 1, 2, \dots, 2N_z$. The integral over \mathbf{k}_{xy} is performed in the first Brillouin zone in the xy reciprocal plane whose surface is Δ . Finally, one obtains for all layers the following matrix equation:

$$\mathbf{M}(\omega) \mathbf{g} = \mathbf{u}. \quad (14)$$

Note that though n runs from 1 to $2N_z$, the matrix \mathbf{M} has the dimension of $4N_z \times 4N_z$ because for each n there are two functions $g(n, n')$ and $f(n, n')$. In the above equation, \mathbf{g} and \mathbf{u} are the column matrices of dimension $4N_z$, which are defined as follows:

$$\mathbf{g} = \begin{pmatrix} g_{1,n'} \\ f_{1,n'} \\ \vdots \\ g_{2N_z,n'} \\ f_{2N_z,n'} \end{pmatrix}, \quad \mathbf{u} = \begin{pmatrix} 2\langle S_1^z \rangle \delta_{1,n'} \\ 0 \\ \vdots \\ 2\langle S_{2N_z}^z \rangle \delta_{2N_z,n'} \\ 0 \end{pmatrix}, \quad (15)$$

and

$$\mathbf{M}(\omega) = \begin{pmatrix} A_1^+ & B_1 & D_1^+ & D_1^- & \cdots & \cdots & \cdots \\ -B_1 & A_1^- & -D_1^- & -D_1^+ & \cdots & \cdots & \cdots \\ C_2^+ & C_2^- & A_2^+ & B_2 & D_2^+ & D_2^- & \cdots \\ -C_2^- & -C_2^+ & -B_2 & A_2^- & -D_2^- & -D_2^+ & \cdots \\ \cdots & \cdots & \cdots & \cdots & \cdots & \cdots & \cdots \\ \cdots & \cdots & \cdots & C_{N_z}^+ & C_{N_z}^- & A_{N_z}^+ & B_{N_z} \\ \cdots & \cdots & \cdots & -C_{N_z}^- & -C_{N_z}^+ & -B_{N_z} & A_{N_z}^- \end{pmatrix}, \quad (16)$$

where for the spin configuration of type I [Fig. 1(a)] one has

$$\begin{aligned} A_n^\pm &= \omega \pm [2J_n \langle S_n^z \rangle Z + 8I_n \langle S_n^z \rangle], \\ B_n &= -2J_n \langle S_n^z \rangle (Z\gamma), \end{aligned} \quad (17)$$

$$C_n^+ = +4J_{n,n-1}\langle S_n^z \rangle \cos \frac{k_y a}{2}, \quad (18)$$

$$C_n^- = -4J_{n,n-1}\langle S_n^z \rangle \cos \frac{k_x a}{2}, \quad (19)$$

$$D_n^+ = +4J_{n,n+1}\langle S_n^z \rangle \cos \frac{k_y a}{2}, \quad (20)$$

$$D_n^- = -4J_{n,n+1}\langle S_n^z \rangle \cos \frac{k_x a}{2}, \quad (21)$$

in which $Z=4$ is the number of in-plane NN, and

$$\gamma = \frac{1}{Z} \left[4 \cos \left(\frac{k_x a}{2} \right) \cos \left(\frac{k_y a}{2} \right) \right].$$

Here, for compactness we have used the following notations:

(i) J_n and I_n are the in-plane interactions. In the present model J_n is equal to $J=-1$. All I_n are set to be $I(<0)$.

(ii) $J_{n,n\pm 1}$ are the interactions between a spin in the n th layer and its neighbor in the $(n\pm 1)$ th layer. Here, we take $J_{n,n\pm 1}=-1$. Of course, $J_{n,n-1}=0$ if $n=1$, $J_{n,n+1}=0$ if $n=2N_z$.

Now, solving $\det(\mathbf{M}) \equiv |\mathbf{M}|=0$, we obtain the spin-wave spectrum ω of the present system. For each \mathbf{k}_{xy} there are $4N_z$ eigenvalues ω , two by two with opposite signs because of the AF symmetry. The solution for the GF $g_{n,n}$ is given by

$$g_{n,n} = \frac{|\mathbf{M}|_n}{|\mathbf{M}|}, \quad (22)$$

with $|\mathbf{M}|_n$ is the determinant made by replacing the n th column of $|\mathbf{M}|$ by \mathbf{u} in Eq. (15). Writing now

$$|\mathbf{M}| = \prod_i [\omega - \omega_i(\mathbf{k}_{xy})], \quad (23)$$

one sees that $\omega_i(\mathbf{k}_{xy})$, $i=1, \dots, 4N_z$, are poles of the GF $g_{n,n}$. Now, we can express $g_{n,n}$ as

$$g_{n,n} = \sum_i \frac{f_n[\omega_i(\mathbf{k}_{xy})]}{[\omega - \omega_i(\mathbf{k}_{xy})]}, \quad (24)$$

where $f_n[\omega_i(\mathbf{k}_{xy})]$ is

$$f_n[\omega_i(\mathbf{k}_{xy})] = \frac{|\mathbf{M}|_n[\omega_i(\mathbf{k}_{xy})]}{\prod_{j \neq i} [\omega_j(\mathbf{k}_{xy}) - \omega_i(\mathbf{k}_{xy})]}. \quad (25)$$

Next, using the spectral theorem which relates the correlation function $\langle S_i^- S_j^+ \rangle$ to the GF [44], one has

$$\langle S_i^- S_j^+ \rangle = \lim_{\epsilon \rightarrow 0} \frac{1}{\Delta} \int \int d\mathbf{k}_{xy} \int_{-\infty}^{+\infty} \frac{i}{2\pi} [g_{n,n}'(\omega + i\epsilon) - g_{n,n}'(\omega - i\epsilon)] \frac{d\omega}{e^{\beta\omega} - 1} e^{i\mathbf{k}_{xy} \cdot (\mathbf{R}_i - \mathbf{R}_j)}, \quad (26)$$

where ϵ is an infinitesimal positive constant and $\beta=1/k_B T$, k_B being the Boltzmann constant.

Using the GF presented above, we can calculate self-consistently various physical quantities as functions of tem-

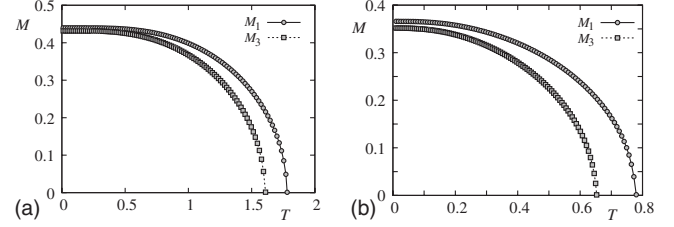


FIG. 13. Magnetization of sublattices 1 (surface) and 3 (second layer) versus temperature for $N_z=2$ and $I=-0.25$ (upper) and $I=-0.01$ (lower).

perature T . Large values of Ising-type interaction I will enhance the ordering. On the contrary, for $I \rightarrow 0$ the transition temperature will go to zero according to the Mermin-Wagner theorem [39]. This is seen in the following. For numerical integration, we will use 80^2 points in the first Brillouin zone.

Figure 13 shows the sublattice magnetizations of the first two layers for $N_z=2$ with $I=-0.25$ and $I=-0.01$ (upper and lower figures, respectively). As seen, the surface sublattice magnetization is larger than the sublattice magnetization of the second layer for $N_z=2$ in qualitative agreement with the MC results shown in Fig. 7, in spite of the fact that due to a finite-size effect, there is a queue of the sublattice magnetization above the transition temperatures for MC results. Note that the AF coupling gives rise to a zero-point spin contraction at $T=0$ which is different for the surface spins and the second-layer spins. We show in Fig. 14 the phase diagram in the space (I, T) where T_1 and T_3 are transition temperatures of the surface sublattice 1 and the sublattice 3 of the second layer.

V. CONCLUDING REMARKS

We have shown in this paper the crossover of the phase transition from first to second order in the frustrated Ising fcc AF film. This crossover occurs when the film thickness N_z is smaller than a value between 2 and 4 fcc lattice cells. These results are obtained with the highly performing Wang-Landau flat histogram technique which allows to determine the first-order transition with efficiency.

For $N_z=2$, we found that in a range of temperature the surface spins stay ordered while interior spins are disordered.

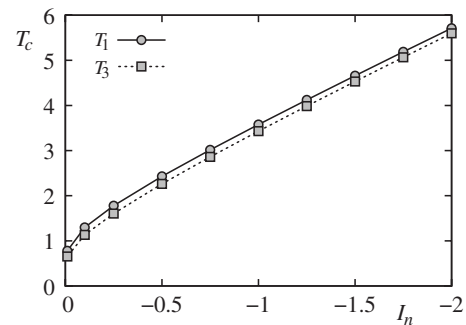


FIG. 14. Phase diagram obtained by the GF method. T_1 and T_3 are transition temperatures of the sublattice 1 of the surface and of the sublattice 3 of the second layer. The transition temperatures should go to zero as $I \rightarrow 0$ (see text).

We interpret this as an effect of the frustration reduction: due to the lack of neighbors, the surface spins are less frustrated than the interior spins. As a consequence, interior spins are disordered at a lower temperature. This has been verified by the Green's function calculation.

The second-order transition for $N_z=2$ is governed by the surface disordering and is characterized by critical exponents whose values are deviated from those of the 2D Ising universality class. We believe that this deviation results from the effect of the disordered interior spins which act as “correlated” random fields on the surface spins. We do not know if the critical exponents found here belong to a new universal-

ity class or they are just “effective critical exponents” which one could scale in some way or another to bring into the 2D Ising universality class. Anyway, these exponents seem to obey a weak universality. An answer to this question is desirable.

ACKNOWLEDGMENT

One of us (V.T.N.) thanks the University of Cergy-Pontoise for financial support and hospitality during the final stage of this work.

-
- [1] X. T. Pham Phu, V. Thanh Ngo, and H. T. Diep, *Surf. Sci.* **603**, 109 (2009).
- [2] T. W. Capehart and M. E. Fisher, *Phys. Rev. B* **13**, 5021 (1976).
- [3] H. T. Diep, M. Debauche, and H. Giacomini, *Phys. Rev. B* **43**, 8759 (1991) rapid communication.
- [4] M. Debauche, H. T. Diep, P. Azaria, and H. Giacomini, *Phys. Rev. B* **44**, 2369 (1991).
- [5] See reviews on theories and experiments given in *Frustrated Spin Systems*, edited by H. T. Diep (World Scientific, Singapore, 2005).
- [6] A. Zangwill, *Physics at Surfaces* (Cambridge University Press, Cambridge, England, 1988).
- [7] *Ultrathin Magnetic Structures*, edited by J. A. C. Bland and B. Heinrich (Springer-Verlag, Berlin, 1994), Vols. I and II.
- [8] H. W. Diehl, in *Phase Transitions and Critical Phenomena*, edited by C. Domb and J. L. Lebowitz (Academic, London, 1986), Vol. 10; H. W. Diehl, *Int. J. Mod. Phys. B* **11**, 3503 (1997).
- [9] M. N. Baibich, J. M. Broto, A. Fert, F. Nguyen Van Dau, F. Petroff, P. Etienne, G. Creuzet, A. Friederich, and J. Chazelas, *Phys. Rev. Lett.* **61**, 2472 (1988).
- [10] P. Grunberg, R. Schreiber, Y. Pang, M. B. Brodsky, and H. Sowers, *Phys. Rev. Lett.* **57**, 2442 (1986); G. Binasch, P. Grunberg, F. Saurenbach, and W. Zinn, *Phys. Rev. B* **39**, 4828 (1989).
- [11] A. Barthélemy *et al.*, *J. Magn. Magn. Mater.* **242-245**, 68 (2002).
- [12] See review by E. Y. Tsymlal and D. G. Pettifor, *Solid State Physics* (Academic Press, San Diego, 2001), Vol. 56, pp. 113–237.
- [13] See V. T. Ngo, H. V. Nguyen, H. T. Diep, and V. L. Nguyen, *Phys. Rev. B* **69**, 134429 (2004) and references on magnetic multilayers cited therein.
- [14] See V. T. Ngo and H. T. Diep, *Phys. Rev. B* **75**, 035412 (2007) and references on surface effects cited therein.
- [15] J. Villain, R. Bidaux, J. P. Carton, and R. Conte, *J. Phys. (Paris)* **41**, 1263 (1980).
- [16] C. L. Henley, *J. Appl. Phys.* **61**, 3962 (1987).
- [17] H. T. Diep and H. Kawamura, *Phys. Rev. B* **40**, 7019 (1989).
- [18] C. Pinettes and H. T. Diep, *J. Appl. Phys.* **83**, 6317 (1998).
- [19] M. K. Phani, J. L. Lebowitz, and M. H. Kalos, *Phys. Rev. B* **21**, 4027 (1980).
- [20] T. L. Polgreen, *Phys. Rev. B* **29**, 1468 (1984).
- [21] D. F. Styer, *Phys. Rev. B* **32**, 393 (1985).
- [22] J. Pommier, H. T. Diep, A. Ghazali, and P. Lallemand, *J. Appl. Phys.* **63**, 3036 (1988).
- [23] A. D. Beath and D. H. Ryan, *Phys. Rev. B* **73**, 174416 (2006).
- [24] M. V. Gvozdkova and M. E. Zhitomirsky, *JETP Lett.* **81**, 236 (2005).
- [25] H. T. Diep, *Phys. Rev. B* **45**, 2863 (1992), and references therein.
- [26] V. Ngo and H. T. Diep, *J. Appl. Phys.* **103**, 07C712 (2008).
- [27] V. T. Ngo and H. T. Diep, *Phys. Rev. E* **78**, 031119 (2008).
- [28] V. Thanh Ngo and H. T. Diep, *J. Phys.: Condens. Matter* **19**, 386202 (2007).
- [29] F. Wang and D. P. Landau, *Phys. Rev. Lett.* **86**, 2050 (2001); *Phys. Rev. E* **64**, 056101 (2001).
- [30] G. Brown and T. C. Schulhess, *J. Appl. Phys.* **97**, 10E303 (2005).
- [31] B. J. Schulz, K. Binder, M. Müller, and D. P. Landau, *Phys. Rev. E* **67**, 067102 (2003).
- [32] A. Malakis, S. S. Martinos, I. A. Hadjiagapiou, N. G. Fytas, and P. Kalozoumis, *Phys. Rev. E* **72**, 066120 (2005).
- [33] Diep-The-Hung, J. C. S. Levy, and O. Nagai, *Phys. Status Solidi B* **93**, 351 (1979).
- [34] Diep-The-Hung, *Phys. Status Solidi B* **103**, 809 (1981).
- [35] Yoseph Imry and Shang-Keng Ma, *Phys. Rev. Lett.* **35**, 1399 (1975).
- [36] H. T. Diep and H. Giacomini, see chapter “Frustration—Exactly Solved Frustrated Models” in Ref. [5].
- [37] A. M. Ferrenberg and D. P. Landau, *Phys. Rev. B* **44**, 5081 (1991).
- [38] M. Suzuki, *Prog. Theor. Phys.* **51**, 1992 (1974).
- [39] N. D. Mermin and H. Wagner, *Phys. Rev. Lett.* **17**, 1133 (1966).
- [40] See for example R. Quartu and H. T. Diep, *Phys. Rev. B* **55**, 2975 (1997).
- [41] C. Santamaria, R. Quartu, and H. T. Diep, *J. Appl. Phys.* **84**, 1953 (1998).
- [42] N. N. Bogolyubov and S. V. Tyablikov, *Dokl. Akad. Nauk SSSR* **126**, 53 (1959) [*Sov. Phys. Dokl.* **4**, 604 (1959)].
- [43] P. Fröbrich, P. J. Jensen, and P. J. Kuntz, *Eur. Phys. J. B* **13**, 477 (2000) and references therein.
- [44] D. N. Zubarev, *Usp. Fiziol. Nauk* **187**, 71 (1960) [*Sov. Phys. Usp.* **3**, 320 (1960)].